Dielectric relaxation, ac and dc conductivities in the fullerenes C_{60} and C_{70}

P. Mondal, P. Lunkenheimer, A. Loidl

Institut für Festkörperphysik, Technische Hochschule Darmstadt, Hochschulstrasse 6, D-64289 Darmstadt, Germany

Abstract. The complex conductivity in polycrystalline C_{60} and C_{70} has been investigated for frequencies 20 Hz $\leq \nu \leq 10^6$ Hz and temperatures 10 K $\leq T \leq$ 750 K. The high-frequency dielectric constants $\varepsilon_\infty = 2.6 \pm 0.1$ (C_{60}) and $\varepsilon_\infty = 4.6 \pm 0.1$ (C_{70}) were deduced from these experiments. The observed low temperature relaxation process in C_{60} fits well into the relaxation dynamics of the C_{60} molecules as determined by many other experimental techniques operating on very different time scales. In addition to the study of the dipolar relaxation process, the dc and ac conductivities were determined. From the temperature dependence of the dc conductivities energy barriers of $E_G = 1.75 \pm 0.1$ eV (C_{60}) and $E_G = 1.7 \pm 0.1$ eV (C_{70}) were estimated. In C_{70} we found indications for small polaron tunneling.

Introduction

The discovery [1] and synthesis of the fullerenes in quantitative amounts [2] have attracted a great deal of activity in the last years concerning the investigation of the solid state properties especially of the two most stable fullerenes, the soccerball-shaped C_{60} and the football-like C_{70}. In the solid state the nearly spherical C_{60} fullerenes rotate almost freely on the sites of a face-centered cubic (f.c.c.) lattice. At about 260 K the crystal transforms to a predominantly orientationally ordered simple-cubic (s.c) structure (space group $Pa\bar{3}$). Hindered reorientational motions of the molecules are observed in this phase and local disorder persists down to lower temperatures [3, 4]. The relaxation dynamics involved were studied by a variety of experimental techniques which operate on vastly different time scales, including ^{13}C-NMR [5], specific heat [6], thermal expansion [7], thermal conductivity [8] and elastic measurements [9]. Very unexpectedly, it was possible to observe the molecular relaxation dynamics in C_{60} also via dielectric spectroscopy [10, 11]. Alers et al. [10] suggested that dipolar moments may be induced by adjacent pairs of misoriented C_{60} fullerenes, as a consequence of the broken inversion symmetry of the orientationally ordered s.c. phase. Due to the difficulties to prepare pure samples much less work was devoted to the statics and dynamics of solid C_{70}. Nevertheless, it is now established that solid C_{70} reveals a completely disordered f.c.c. or h.c.p. (hexagonal-closed-packed) rotator phase for temperatures above $T \approx 350$ K. Between $T \approx 350$ K and $T \approx 280$ K, C_{70} exhibits a rhombohedral structure with the long molecular axes along one of the $\langle 111 \rangle$ directions and hindered reorientational motions about these axes. The transition between these two phases reveals a large thermal hysteresis (≈ 50 K). A second phase transition into a monoclinic structure occurs roughly at 280 K. In this low temperature phase no reorientational motion of the fullerenes could be detected [12–16].

In the present investigation the dielectric constant and the conductivity of polycrystalline samples of C_{60} and C_{70} were studied in a broad frequency and temperature range. By investigating samples which have been exposed to various annealing procedures we tried to clarify the question whether the dipolar moment in C_{60} is an intrinsic property of the fullerite or wether it is caused by impurities, e.g. by oxygen which is easily absorbed on C_{60} [17]. We compare our results on the dipolar relaxation dynamics in C_{60} with the reorientation times obtained from other experimental techniques [5–9] and classify the freezing process in Angell's scheme for "strong" and "fragile" glassformers [18]. We address the question wether the hindering barriers are determined exclusively by the lattice anisotropy or wether multipolar exchange interactions play the dominant role. For the latter case experimental indications are often inferred from the observation of polydispersive relaxation behaviour or from deviations from a simple Arrhenius-type slowing down of the relaxation times [19]. For C_{70} to our knowledge there have been no dielectric measurements reported up to now and it would be highly interesting to find out if dipolar relaxation effects similar to those observed in C_{60} can be detected. In addition we present a detailed investigation of the complex conductivity in

C_{60} and C_{70}. We find hopping of localized charge carriers as the dominant mechanism of charge transport in C_{70} and compare our results to the predictions of various hopping models.

Experimental details

The real and imaginary parts of the complex dielectric constant were recorded in the frequency range 20 Hz $\leq \nu \leq 10^6$ Hz using the autobalance bridge HP 4284 A. To carry out temperature dependent measurements the samples have been mounted in a helium refrigerator system ($15\ \mathrm{K} \leq T \leq 300\ \mathrm{K}$) and in an oven ($300\ \mathrm{K} \leq T \leq 750\ \mathrm{K}$), respectively. The samples were prepared using commerical C_{60} and C_{70} powders of "gold grade" purity which were pressed into pellets under a pressure of 0.3 GPa. They had a typical size of $\varnothing$ 6 mm × 0.2 mm which corresponds to a geometrical capacity of approximately 1.25 pF. The pellets were inserted between polished brass plates and were repeatedly heated in vacuum from room temperature to 750 K to remove residual solvents and other impurities. This procedure was terminated when the simultaneously measured conductivity σ(T) yielded reproducible results. Anomalies due to the structural phase transition of C_{60} showed up in the real and imaginary part of the complex dielectric constant only after such annealing treatments. To study a possible dependence of the observed dipolar effects in C_{60} on the oxygen content the samples were annealed in oxygen atmospheres of 2 bar pressure for several days.

Results

Representative measurements of the temperature and frequency dependence of the dielectric function of C_{60} are presented in Fig. 1. It shows the real and imaginary part of the complex dielectric constant $\varepsilon^* = \varepsilon' + i\varepsilon''$ for different measuring frequencies in the temperature range from 15 K to 300 K. At 260 K frequency independent discontinuities in the real and imaginary part of ε^* (indicated by arrows) provide clear experimental evidence for the structural phase transition from the orientationally disordered f.c.c. phase to the orientationally ordered s.c. phase. At the phase transition temperature ε' reveals an abrupt increase of 0.4%. It can be attributed to a contraction of the lattice constant in good agreement with results from neutron diffraction [4] and dilatometry experiments [7]. Frequency dependent anomalies appear between 130 K and 200 K with a steplike decrease in ε' and a corresponding peak in ε''. The temperatures of the points of inflexion in ε' and of the maxima in ε'' decrease with decreasing frequency. Such a behavior is typical for the freezing of orientational degrees of freedom on the time scale given by the frequency of the exciting field and has already been observed by Alers et al. [10] in single crystals of C_{60}. In the following this relaxation will be called the low temperature relaxation. At temperatures $T < 100$ K the high frequency limit of ε' can be determined as $\varepsilon_\infty = 2.60 \pm 0.01$. The height of the relaxation step, i.e. the reorientational dipolar contribution to ε' is about 0.015.

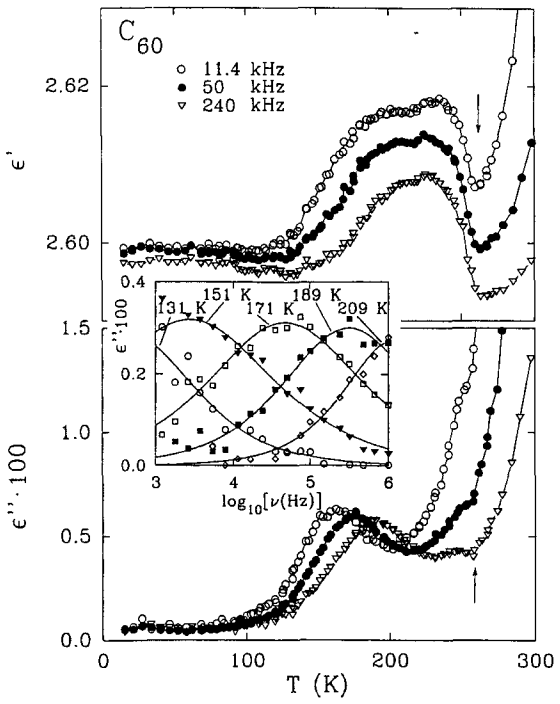

Fig. 1. Temperature dependence of the real and the imaginary parts of the dielectric function in C_{60}. Upper frame: $\varepsilon'(T)$ at three frequencies as listed in the figure. Lower frame: $\varepsilon''(T)$ for the same three frequencies. The arrows indicate the phase transition temperature. The inset shows the frequency dependence of $\varepsilon''(\omega)$ for several temperatures obtained by subtracting a linear (in T) conductivity background. The lines are the results of a fit using a Cole–Cole distribution of relaxation times

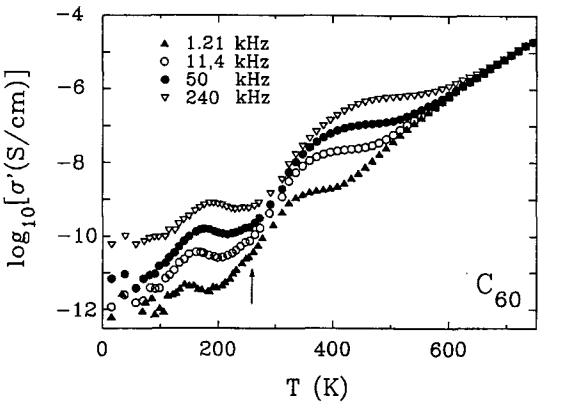

Fig. 2. Temperature dependence of the real part of the conductivity in C_{60} at four measuring frequencies as listed in the figure. The arrow indicates the phase transition temperature

The relaxation feature as detected in the dielectric loss is superimposed on conductivity contributions. To study those in more detail the real part of the complex conductivity, $\sigma' = \varepsilon_0 2\pi\nu\varepsilon''$, is shown in Fig. 2 for the same C_{60} sample for frequencies between 1.21 kHz and 240 kHz in the complete temperature region investigated. Below 90 K, nearly temperature independent ac conductivities dominate followed by the low temperature relaxation

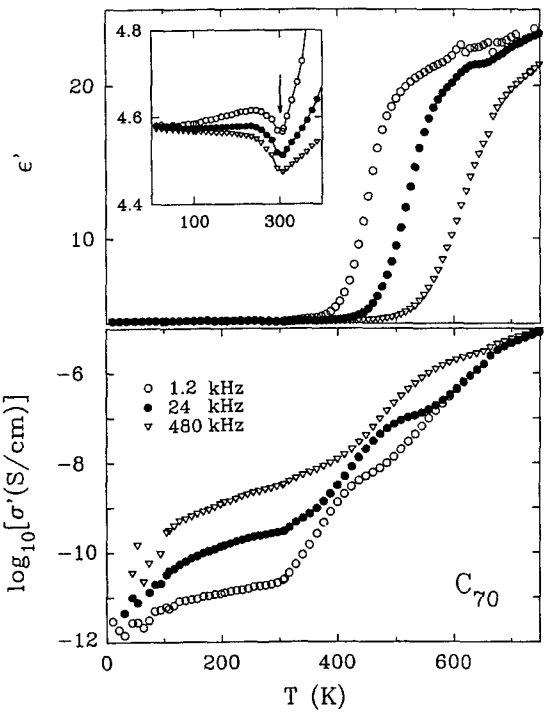

Fig. 3. Temperature dependence of the real part of the dielectric function and the real part of the conductivity $\sigma' = \varepsilon_0 \omega \varepsilon''$ in C_{70} at three frequencies. Inset: $\varepsilon'(T)$ in the low temperature region. The arrow indicates the phase transition temperature

which is superimposed on a strongly temperature dependent ac conductivity. Between 200 K and 300 K the frequency dependence is again mainly due to ac conductivity contributions. The arrow marks the structural phase transition. At higher temperatures another relaxation feature shows up which will be called the high temperature relaxation in the following. For $T \geq 500$ K the 1.21 kHz curve approximately represents the pure dc conductivity.

The temperature dependence of the real parts of the dielectric constant ε' and of the conductivity σ' of C_{70} are presented in Fig. 3 for three measuring frequencies and temperatures $10\ \text{K} \leq T \leq 750$ K. In the low temperature region, $T < 300$ K, ε' (see inset) and σ' reveal no evidence for relaxation processes. This observation is in agreement with neutron diffraction data [12, 14] which showed no molecular reorientations below room temperature. In this temperature range ac conductivity dominates which finally vanishes for $T \to 0$. At the lowest temperatures ε' is only determined by its high frequency limit, $\varepsilon_\infty = 4.6 \pm 0.1$. At 300 K and on heating, frequency independent steps in ε' indicate a phase transition. Upon cooling this transition occurs at temperatures approximately 30 K lower. This large thermal hysteresis gives reason for the assumption that it is the transition from the f.c.c. to the rhombohedral phase although it has been observed previously at significantly higher temperatures [12–16]. McGhie et al. [15] investigated the dependence of this phase transition temperature on the C_{60} content of the samples. From their results one has to conclude that the content of C_{60} in our samples was larger than 2%. The chemical analysis yielded a C_{60} content of 1%. On the other hand Meingast et al. [16] observed another transition at 300 K which they attribute to the freezing in of precessional motion of the long molecular axes in the rhombohedral phase. This transition is less distinctive than the transition from the f.c.c. into the rhombohedral phase and reveals a much smaller thermal hysteresis. Moreover, the transition f.c.c. to rhomobohedral is accompanied by a large decrease of the crystal axes (c-axis $\approx 6\%$, a-axis $\approx 2.5\%$ [16]) which could explain the steplike increase of ε' of 2% observed in our measurements. The transition from the rhombohedral to the monoclinic phase is accompanied by a change of the lattice parameters of only 0.4–0.8% [16]. Therefore, we think that the phase transition which we observed between 270 K and 300 K indicates rather the transition from the f.c.c. to the rhombohedral phase than that from the rhombohedral to the monoclinic phase or than the freezing-in of precessional motion of the long molecular axes in the rhombohedral phase. For $T \geq 300$ K and similar to our findings in C_{60}, both ε' and ε'' exhibit frequency dependent anomalies which are characteristic for dipolar relaxations. At the highest temperatures investigated ($T \geq 500$ K), the dc conductivity dominates over the ac conductivity as can be seen from the identical shapes and values of the 1.2 kHz and the 24 kHz curves.

Discussion

In order to analyse the low temperature relaxation in C_{60} the conductivity background was subtracted from the imaginary part of the dielectric function in the low temperature region shown in Fig. 1. The frequency dependence of the resulting loss peaks is shown in the inset of Fig. 1 for various temperatures. The peaks exhibit half widths of $W = 2.3 \pm 0.3$ decades which are significantly broader than for a Debye relaxator characterized by a width $W = 1.14$ decades. This finding indicates the presence of a distribution of relaxation times and can be compared to the results of Alers et al. [10] on single crystals of C_{60}. These authors analysed $\varepsilon'(T)$ for $150\ \text{K} \leq T_r \leq 180$ K by assuming a Gaussian distribution of activation energies with a full width at half minimum (FWHM) of $\Sigma = 68$ meV. The width of the corresponding distribution of relaxation times is given by $W = \Sigma/(k_B T_r \ln 10)$ [20] and yields $W = 2.2 \pm 0.3$ decades (see Ref. [11]). Hence the width of the loss peaks as obtained from the experiments on single crystals is consistent with the width from our study on polycrystalline C_{60}. Because of that correspondence it can be excluded that the broadening of the loss peaks is caused by effects of grain boundaries. The solid lines in the inset of Fig. 1 represent least square fits for a Cole-Cole distribution of relaxation times:

$$\varepsilon^* = \varepsilon_\infty + \frac{\varepsilon_s - \varepsilon_\infty}{1 + (i\omega\tau_0)^{1-\alpha}}. \tag{1}$$

The fits yield a mean value for the broadening parameter of $\alpha = 0.32$. The second fit parameter $\varepsilon_s - \varepsilon_\infty = 0.011 \pm 0.003$ represents the contribution of the dipoles to ε' which is in agreement with the value of about 0.015 estimated

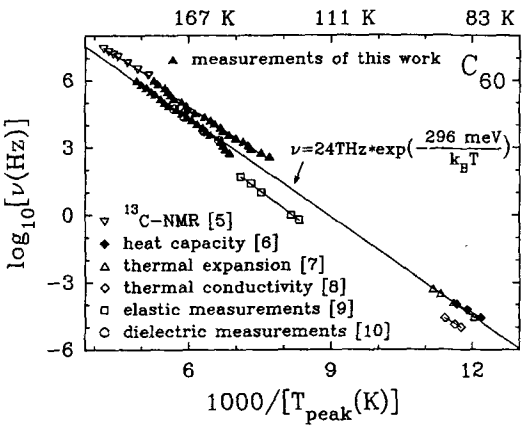

Fig. 4. Logarithm of the mean relaxation rates versus the inverse temperature in C_{60}. Full triangles: dielectric results of the present investigation for two different polycrystalline samples. Other symbols: results of relaxation dynamics observed with other experimental techniques as listed in the figure. The dielectric results of Alers et al. [10] in C_{60} single crystals are also shown (open circles)

previously. Since it has been reported that oxygen is easily absorbed by C_{60} [17], we analysed the influence of oxygen on the broadening and height of the relaxation peaks. The dielectric function was measured again after annealing the same sample under an oxygen atmosphere of 2 bars for 91 hours. The subsequent measurements revealed negligible changes in the width and the height of the relaxation peaks. Therefore, we conclude that the oxygen content of the sample is neither responsible for the dipole moment nor the distribution of relaxation times. This finding supports the suggestion of Alers et al. [10] that the dipole moment in C_{60} has an intrinsic origin: In the orientationally ordered s.c. phase with $Pa\bar{3}$ symmetry double bonds of one molecule face pentagons of its nearest neighbor molecules and both, the molecule and the lattice, have inversion symmetry and does not allow a permanent dipole to exist. As there has been found local disorder in this phase [3,4] a dipole moment may be induced on the neighbors of a misoriented molecule (double bonds face hexagons of the nearest neighbors) as a result of the broken inversion symmetry on the neighboring sites. In order to contribute to the dielectric susceptibility the neighboring dipole has to reorient in response to an applied electric field introducing a second misorientated molecule. Hence, a two-defect model is required to generate the dielectric response.

The mean relaxation times of the low temperature relaxation in C_{60} were determined from the conductivity-corrected $\varepsilon''(T)$ in Fig. 1. In Fig. 4 the logarithm of the mean relaxation rate is plotted versus the inverse temperature for two different samples (filled triangles). The temperature dependence of the mean relaxation rates ν_m as determined from both experiments clearly follows an Arrhenius law

$$\nu_m = \nu_0 \exp(-E_B/(K_B T)). \quad (2)$$

The energy barriers, E_B, against reorientations and the attempt frequencies, ν_0, vary from 293 meV to 306 meV and from 20 THz to 80 THz to 80 THz, respectively. But despite these discrepancies, Fig. 4 provides clear experimental evidence that the dielectric relaxation rates of the low temperature relaxation are consistent with the Arrhenius behaviour of the inverse time constants as determined by different experimental techniques, covering 12 decades of measuring frequencies [10], [5–9]. Thus, all experiments albeit operating on very different time scales measure the same thermally activated reorientation process of the C_{60} fullerenes. The results of measurements of the elastic relaxation [9] and the of the time dependent thermal expansion [7] in C_{60} could be satisfactorily described using a single relaxation time, in clear contrast to our results on polycrystalline samples and to the dielectric results of Alers et al. [10] on single crystals. These discrepancies can hardly be understood due to the fact that the temperature dependence of the mean relaxation rates proofs that these different techniques probe the same unique relaxation process and that it is generally believed that the reorientational motion is dominated by single-particle processes. The only way out of these difficulties lies in the assumption that the Gaussian width of the distribution of energy barriers decreases with decreasing temperatures and hence, that the experiments operating at lower measuring frequencies see almost a Debye behavior of the reorientating molecules. This has to be prooven experimentally and we try to conduct dielectric experiments at frequencies below the Hz regime. The best guess for the parameters of the underlying Arrhenius law which determines the universal temperature dependence of the relaxation rates is given by $\nu_0 = 24 \pm 20$ THz and $E_B = 296 \pm 20$ meV. The slowing down of the relaxation rate in C_{60} is similar to that observed in many orientational glasses and plastic crystals [19]. Like those, C_{60} can be classified as a "strong liquid" in Angell's schema for glass forming materials [18]. The observed relaxation behavior supports the thesis that the polydispersive relaxation behavior observed in C_{60} is caused by random fields and not by multipolar exchange interactions. Moreover, in systems governed by thermally activated dynamics deviations from Debye behavior are often due to the presence of static random fields [19].

At the order-disorder phase transition temperature T_c the mean relaxation rate is 44 MHz. Above T_c the relaxation rate is strongly enhanced and the hindering barrier against molecular reorientations is significantly reduced to approximately 35–46 meV, which follows from X-ray and neutron diffraction experiments [21,22]. The temperature dependence of the mean relaxation rates of the high temperature relaxation in C_{60}, shown in Fig. 2, also follows an Arrhenius law with an energy barrier $E_B \approx 514$ meV and an attempt frequency $\nu_0 \approx 480$ GHz. This energy barrier is incompatible with the 35–46 meV found in the diffraction experiments. Hence it seems questionable if the high temperature relaxation observed in this work is an intrinsic phenomenon. Possibly it arises from solvent residuals or fullerene derivatives which may be produced in the first heating cycles.

The high temperature relaxation in C_{70} (see Fig. 3) also reveals Arrhenius behavior for the temperature dependence of the mean relaxation rates. The energy barrier $E_B \approx 870$ meV again is not in agreement with the reorientational dynamics in C_{70} observed with other

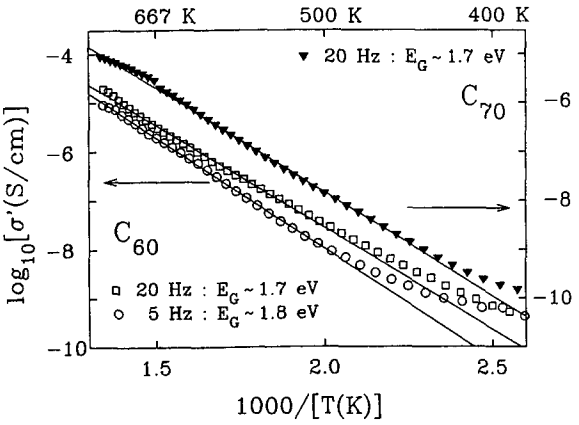

Fig. 5. Logarithm of the real part of the conductivity in C_{60} for two different samples (open symbols, left scale) and in C_{70} (closed symbols, right scale) recorded at 5 Hz and 20 Hz, respectively, versus the inverse temperature. The solid lines are the results of fits using the Arrhenius law

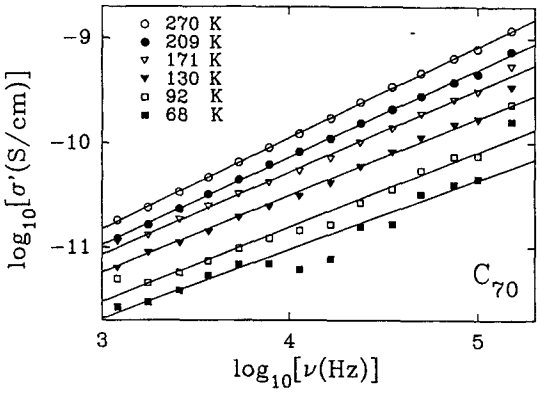

Fig. 6. Logarithm of the real part of the conductivity σ' versus the logarithm of the measuring frequency ν in C_{70} for temperatures 70 K < T < 300 K. In this double logarithmic plot straight lines with a slope smaller unity result, a clear evidence for hopping conductivity. The solid lines are the results of a fit with $\sigma' \propto \nu^s$

experimental techniques: above 345 K the diffraction experiments give evidence for an almost free rotation of the C_{70} molecules about arbitrary axes [12, 14]. Therefore, also in C_{70} the intrinsic nature of the high temperature relaxation observed in our experiments seems questionable. But we have to state clearly that we observed the high temperature relaxations in all C_{60} and C_{70} samples independent of sample history or sample treatment.

Finally, we would like to analyse the experimentally observed ac and dc conductivities in more detail. The temperature dependence of the real part of the conductivity σ' in C_{60} and C_{70} has been shown in Fig. 2 and Fig. 3. In both compounds the dc conductivity dominates at high temperatures (above the high temperature relaxations). In Fig. 5 σ' is plotted in Arrhenius representation for two different C_{60} samples and one C_{70} sample as measured at 5 Hz and 20 Hz, respectively. Above 450 K the data exhibit a linear behavior characteristic for a purely thermally activated conductivity. From the slopes of the straight lines band gaps for the two C_{60} samples, $E_G = 1.7 \pm 0.1$ eV and $E_G = 1.8 \pm 0.1$ eV, have been estimated. For the energy gap in C_{70} we found $E_G = 1.7 \pm 0.1$ eV. These results are in fair agreement with the trend given by theoretical values for the energy gap between the highest occupied molecular orbital (HOMO) and the lowest unoccupied molecular orbital (LUMO) of the C_{60} and C_{70} fullerenes: Saito et al. calculated HOMO–LUMO splittings for C_{60} of 1.9 eV [23] and C_{70} of 1.65 eV [24] using local density approximations. They also predicted a direct band gap in C_{60} at the Brillouin zone boundary (X point), $E_G = 1.5$ eV, [23] which is smaller than the HOMO–LUMO splitting due to the broadening of the energy levels. In various optical measurements (emission and absorption) the optical gap in C_{60} has been observed in the range 1.7 eV–1.9 eV [25–28]. From electron energy-loss spectroscopy (EELS) [29] a value of the band gap, $E_G = 2.1$ eV, has been deduced. From thin film conductivity measurements Mort et al. estimated a band gap of 1.9 eV [30]. The same value was determined in a microwave conductivity study [31]. Besides the EELS result all these values are in agreement with our results for the gap in C_{60}. Considerably less information is available about the band gap in C_{70}; as indicated by the theoretical studies it is expected to be smaller than the gap in C_{60}. This trend seems to be underlined by optical measurements of $\varepsilon(\omega)$ [32] and microwave conductivity measurements [31] which resulted in 1.25 eV and 1.57 eV, respectively. These findings are compatible with our result within the error bars. Results from EELS [29] for C_{70}, $E_G = 2$ eV, again seem to be to high in comparison with the values determined by the other experimental techniques. Finally, we want to remark that the high temperature dc conductivity measures the intrinsic current created by thermal activation of charge carriers over the band gap. However, as there are indications for the formation of small polarons in C_{70}, as shown below, it is possible that the optical excitation energy is larger than the band gap found in transport measurements. For the optical excitation the charge carrier must overcome its polaronic binding energy in addition to its delocalisation energy while in transport measurements the lattice has time to relax and the polaronic binding energy does not contribute to the activation energy.

The ac conductivity can only be investigated at temperatures and frequencies were it dominates over the dc conductivity and relaxation processes. For C_{60} this regime is limited to temperatures below 100 K. Here the quality of the data is too low to allow for a quantitative analysis. On the other hand, in C_{70} the ac conductivity dominates below 300 K and for a more detailed examination of the responsible conduction process the frequency dependence of the real part of the conductivity σ' is shown in Fig. 6 for various temperatures. In the double logarithmic plot of Fig. 6 straight lines result with slopes smaller unity. This frequency dependence of σ' can be parameterized according to $\sigma' \propto \omega^s$, a characteristic feature of hopping of charge carriers in amorphous semiconductors or between localized defect states in crystalline semiconductors [33–35]. However, it can also arise by a distribution of capacitive junctions in the sample which may be

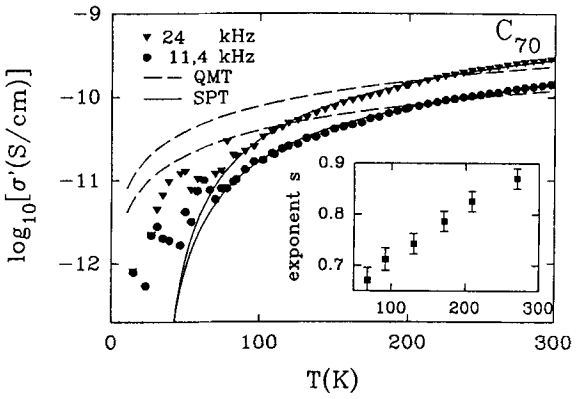

Fig. 7. Temperature dependence of the logarithm of the real part of the conductivity in C_{70} at two frequencies as listed in the figure. The lines are the results of fits using the model of quantum-mechanical tunneling of electrons (QMT) and of small-polaron tunneling (SPT), respectively. Inset: Temperature dependence of the frequency exponent s obtained from the slopes of the straight lines in Fig. 5

due to cracks or grain boundaries. We checked this by investigating various samples which have been subjected to different milling procedures and pressures during the preparation of the pellets. In addition, the samples were also annealed in oxygen or in vacuum to exclude the oxygen as the origin of the defect states. The ac conductivities in all samples behaved very similar which points to the intrinsic nature of the hopping conduction in C_{70}. However, from our experiments it is difficult to make a statement about the origin of the defect states that lead to the hopping conduction in C_{70}. Having in mind these uncertainties, in the following we want to analyze the ac conductivity in C_{70} in more detail. Besides the frequency dependence the models for hopping conductivity make distinct predictions concerning the temperature dependence of the ac conductivity. We therefore fitted the temperature dependence of the conductivity $\sigma'(T)$ by using the predictions of different models of hopping conductivity including the quantum-mechanical tunneling model (QMT) and the small-polaron tunneling model (SPT) [33, 34]. The best results were achieved using the model for small-polaron tunneling which are shown in Fig.7 as solid lines. A characteristic relaxation time of $1.5 \cdot 10^{-13}$s and an activation energy for the polaron transport of 45 meV result as parameters from these fits. The temperature dependence of the exponent s which has been deduced from the slopes of the straight lines in Fig. 6 is shown in the inset of Fig. 7. It corresponds qualitatively to the temperature dependence predicted by the model for small-polaron tunneling but in this model s is limited to values smaller than 0.8, at least for a reasonable choice of parameters, while s as determined from the present experiments on C_{70} clearly reaches higher values. However, no other model was able to give a nearly as good description of the experimental results (see e.g. dashed lines in Fig. 7 which were calculated using the predictions of the QMT model). Hence, we assume small polaron tunneling as the most probable ac conduction mechanism in C_{70} although the origin of the defect states is still unclear at the moment. The existence of polarons in C_{70} can possibly be understood in a similar way as reported for C_{60} as on-ball excitations of the fullerenes [36, 37].

Conclusion

We have measured the dielectric function of C_{60} and C_{70} powders in the frequency range from 20 Hz to 10^6 Hz and for temperatures between 10 K and 750 K.

The measurements on C_{60} revealed clear evidence for the structural phase transition at 260 K. From the steplike increase of ε' at the phase transition temperature it is possible to infer a contraction of the lattice constant of about 0.4% in good agreement with neutron diffraction and dilatometry results [4, 7]. The high frequency dielectric constant of C_{60} was determined to be $\varepsilon_\infty = 2.6 \pm 0.1$.

In addition, we observed an intrinsic dipolar relaxation in C_{60} similar to that found in single crystals [10]. The dielectric mean relaxation rates exhibit Arrhenius behavior with an energy barrier of 290–310 meV and an attempt frequency of 20–70 THz and are consistent with results obtained by other experimental techniques over a range of twelve decades in frequency. The loss peaks exhibit a width of 2.3 ± 0.3 decades in the frequency domain, pointing towards the presence of random fields.

Measurements on C_{70} provided evidence for a structural phase transition at 300 K, which we attribute to the transition from the f.c.c. to the rhombohedral phase which was identified in structural measurements [12–14]. We deduced a high frequency dielectric constant, $\varepsilon_\infty = 4.6 \pm 0.1$. In C_{70} no evidence of dipolar relaxations have been found in the low temperature range.

The dc conductivities in C_{60} as well as in C_{70} follow a purely thermally activated behavior. The energy gaps have been determined as $E_G = 1.75 \pm 0.1$ for C_{60} and $E_G = 1.7 \pm 0.1$ for C_{70}.

The ac conductivity of both fullerites gives clear evidence for hopping of charge carriers between localized defect states the origin of which is unclear at the moment. In C_{70} the ac conductivity was qualitatively analyzed and could be described using a model for small-polaron tunneling.

This research was supported by the Sonderforschungsbereich 262. We thank R. Böhmer for useful and illuminating discussions.

References

1. Kroto, H.W., Heath, J.R., O'Brien, S.C., Curl, R.F., Smalley, R.E.: Nature **318**, 162 (1985)
2. Krätschmer, W., Lamb, L.D., Fostiropoulos, K., Huffman, D.R.: Nature **347**, 354 (1990)
3. Heiney, P.A., Fischer, J.E., McGhie, A.R., Romanow, W.J., Denenstein, A.M., McCauley, J.P., Smith, A.B., Cox, D.E.: Phys. Rev. Lett. **66**, 2911 (1991)
4. David, W.I.F., Ibberson, R.M., Dennis, T.J.S., Hare, J.P., Prassides, K.: Europhys. Lett. **18**, 219 (1992)
5. Tycko, R., Dabbagh, G., Flemming, R.M., Haddon, R.C., Makhija, A.V., Zahurak, S.M.: Phys. Rev. Lett. **67**, 1886 (1991)
6. Matsuo, T., Suga, H., David, W.I.F., Ibberson, R.M., Bernier, P., Zahab, A., Fabre, C., Rassat, A., Dworkin, A.: Solid State Commun. **83**, 711 (1992)

7. Gugenberger, F., Heid, R., Meingast, C., Adelmann, P., Braun, M., Wühl, H., Haluska, M., Kuzmany, H.: Phys. Rev. Lett. **69**, 3774 (1992)
8. Yu, R.C., Tea, N., Salamon, M.B., Lorents, D., Malhotra, R.: Phys. Rev. Lett. **68**, 2050 (1992)
9. Schranz, W., Fuith, A., Dolinar, P., Warhanek, H., Haluška, M., Kuzmany, H.: Phys. Rev. Lett. **71**, 1561 (1993)
10. Alers, G.B., Golding, B., Kortan, A.R., Haddon, R.C., A. Theil, F.: Science **257**, 5116 (1992)
11. Mondal, P., Lunkenheimer, P., Böhmer, R., Loidl, A.: J. Non-Cryst. Solids **172–174**, 468 (1994)
12. Vaughan, G.B.M., Heiney, P.A., Fischer, J.E., Luzzi, D.E., Ricketts-Foot, D.A., McGhie, A.R., Hui, Y.W., Smith, A.L., Cox, D.E., Romanow, W.J., Allen, B.H., Coustel, N., McCauley, J.P. Jr., Smith, A.B. III: Science **254**, 1350 (1991)
13. Verheijen, M.A., Meekes, H., Meijer, G., Bennema, P., de Boer, J.L., van Smallen, S., Van Tendeloo, G., Amelinckx, S., Muto, S., van Landuyt, J.: Chem. Phys. **166**, 287 (1992)
14. Vaughan, G.B.M., Heiney, P.A., Cox, D.E., Fischer, J.E., McGhie, A.R., Smith, A.L., Strongin, R.M., Chichy, M.A., Smith, A.B. III: Chem. Phys. **178**, 599 (1993)
15. McGhie, A.R., Fischer, J.E., Heiney, P.A., Stephens, P.W., Cappalletti, R.L., Neumann, D.A., Mueller, W.H., Mohn, H., ter Meer, H.-U.: Phys. Rev. B **49**, 12614 (1994)
16. Meingast, C., Gugenberger, F., Roth, G., Haluška, M., Kuzmany, H.: Z. Phys. B **95**, 67 (1994)
17. Werner, H., Bublak, D., Göbel, U., Henschke, B., Bensch, W., Schlögl, R.: Angew. Chem. **104**, 909 (1992)
18. Angell, C.A.: J. Non-Cryst. Solids **13**, 131 (1991)
19. Loidl, A., Böhmer, R. in: Disorder Effects on Relaxational Processes, 659–696. eds. R. Richert and A. Blumen, Berlin, Heidelberg: Springer 1994. Höchli, U. T., Knorr, K., Loidl, A.: Adv. Phys. **39**, 405 (1990)
20. Böhmer, R.: J. Chem. Phys. **91**, 3111 (1989)
21. Neumann, D.A., Copley, J.R.D., Cappelletti, R.L., Kamitakahara, W.A., Lindstrom, R.M., Creegan, K.M., Cox, D.M.W., Romanow, J., Coustel, N., McCauley, J.P. Jr., Maliszewskyj, N.C., Fischer, J.E., Smith, A.B. III: Phys. Rev. Lett. **67**, 3808 (1991)
22. Axe, J.D., Moss, S.C. and Neumann, D.A.: Solid State Phys. **48**, 150 (1994)
23. Saito, S., Oshiyama, A.: Phys. Rev. Lett. **66**, 2637 (1991)
24. Saito, S., Oshiyama, A.: Phys. Rev. B **44**, 11532 (1991)
25. Weaver, J.H., Martins, J.L., Komeda, T., Chen, Y., Ohno, T.R., Kroll, G.H. and Troullier, N., Haufler, R.E., Smalley, R.E.: Phys. Rev. Lett. **66**, 1741 (1991)
26. Kelly, M. K., Etchegoin, P., Fuchs, D.: Phys. Rev. B **46**, 4963 (1992)
27. Guizetti, G., Marabelli, F., Patrini, M., Capozzi, V., Lorusso, G.F., Minafra, A., Manfredini, M., Milani, P.: Phys. Status. Solidi. (b) **183**, 267 (1994)
28. Kazaoui, S., Ross, R., Minami, N.: Solid State Commun. **90**, 623 (1994)
29. Sohmen, E., Fink, J., Krätschmer, W.: Z. Phys. B **86**, 87 (1992)
30. Mort, J., Ziolo, R., Machonkin, M., Huffman, D.R., Freguson, M.I.: Chem. Phys. Lett. **186**, 284 (1991)
31. Rabenau, T., Simon, A., Kremer, R.K., Sohmen, E.: Z. Phys. B. **90**, 69 (1993)
32. Ren, S.-L., Wang, K.A., Zhou, P., Wang, Y., Rao, A.M., Meier, M.S., Selegue, J.P., Eklund, P.C.: Appl. Phys. Lett. **61**, 124 (1992)
33. Elliot, S.R.: Adv. Phys. **36**, 135 (1987)
34. Long, A.R.: Adv. Phys. **31**, 553 (1982)
35. Jonscher, A.K.: Dielectric Relaxation in Solids. London: Chelsea Dielectric Press 1983
36. Matus, M., Kuzmany, H., Sohmen, E.: Phys. Rev. Lett. **68**, 2822 (1992)
37. Salkola, M.I.: Phys. Rev. B **49**, 9533 (1994)